

# APPENDIX

## Assessing U.S. Aggregate Fluctuations Across Time and Frequencies\*

Thomas A. Lubik  
Federal Reserve Bank of Richmond<sup>†</sup>

Christian Matthes  
Federal Reserve Bank of Richmond<sup>‡</sup>

Fabio Verona  
Bank of Finland<sup>§</sup>

February 2019  
Working Paper No. 19-06

---

\*The views expressed in this paper are those of the authors and should not be interpreted as those of the Federal Reserve Bank of Richmond, the Federal Reserve System, or the Bank of Finland.

<sup>†</sup>Research Department, P.O. Box 27622, Richmond, VA 23261. Email: thomas.lubik@rich.frb.org.

<sup>‡</sup>Research Department, P.O. Box 27622, Richmond, VA 23261. Email: christian.matthes@rich.frb.org

<sup>§</sup>Monetary Policy and Research Department. Snellmaninaukio, PO Box 160, 00101 Helsinki. Email: fabio.verona@bof.fi.

## A Some Background on Wavelets

### A.1 Continuous Wavelet Transform

A wavelet  $\psi(t)$  is a function of finite length that oscillates around the time axis. The name wavelet (small wave) derives from the admissibility condition, which requires the mother wavelet to be of finite support (i.e., small) and of oscillatory (wavy) behavior. The most commonly used mother wavelet in economic applications - and the one we use in this paper - is the Morlet wavelet defined by  $\psi(t) = \pi^{\frac{1}{4}} e^{6it} e^{-\frac{t^2}{2}}$ . The continuous wavelet transform of a time series  $x(t)$  with respect to a given mother wavelet is:

$$W_x(\tau, s) = \frac{1}{\sqrt{s}} \int_{-\infty}^{+\infty} x(t) \overline{\psi} \left( \frac{t - \tau}{s} \right) dt, \quad (\text{A.1})$$

where  $\overline{\psi}$  denotes the complex conjugate of  $\psi$ , and  $\tau$  and  $s$  are the two control parameters of the continuous wavelet transform (CWT). The location parameter  $\tau$  determines the position of the wavelet along the time axis, while the scale parameter  $s$  defines how the mother wavelet is stretched. The scale is inversely related to frequency  $f$ , with  $f \approx 1/s$ . A lower (higher) scale means a more (less) compressed wavelet which allows to detect higher (lower) frequencies of the time series  $x(t)$ . The ability and flexibility to endogenously change the length of the wavelets is one of the main advantages of the wavelet transform when compared with the most common alternative, the short-time Fourier transform. The wavelet power spectrum (WPS) of  $x(t)$  is defined as  $(WPS)_x(\tau, s) = |W_x(\tau, s)|^2$ . It measures the local variance distribution of the time series  $x(t)$  around each time and scale/frequency. The WPS can be averaged over time so that it can be compared to classical spectral methods. In particular, the global wavelet power spectrum (GWPS) can be obtained by integrating the WPS over time:  $(GWPS)_x(s) = \int_{-\infty}^{+\infty} W_x(\tau, s) d\tau$ .

### A.2 Maximal Overlap Discrete Wavelet Transform and Wavelet Multiresolution Analysis

Wavelet multiresolution analysis (MRA) allows decomposition of any variable into a trend, a cycle, and a noise component, irrespective of its time series properties. This is similar to the traditional time series trend-cycle decomposition approach (Beveridge and Nelson, 1981, and Watson, 1986) or other filtering methods like the Hodrick and Prescott (1997) or the Baxter and King (1999) band-pass filter. We employ a particular version of the wavelet transform called the Maximal Overlap Discrete Wavelet Transform (MODWT). To perform the MODWT of a given time series, we need to apply an appropriate cascade of wavelet

filters, which is similar to filtering by a set of band-pass filters. This procedure allows us to capture fluctuations from different frequency bands. By using the Haar wavelet filter, any variable  $X_t$ , regardless of its time series properties, can be decomposed as:

$$X_t = \sum_{j=1}^J D_{j,t} + S_{J,t}, \quad (\text{A.2})$$

where the  $D_{j,t}$  are the wavelet coefficients at scale  $j$ , and  $S_{J,t}$  is the scaling coefficient. These coefficients are given by:

$$D_{j,t} = \frac{1}{2^j} \left( \sum_{i=0}^{2^{j-1}-1} X_{t-i} - \sum_{i=2^{j-1}}^{2^j-1} X_{t-i} \right), \quad (\text{A.3})$$

$$S_{J,t} = \frac{1}{2^J} \sum_{i=0}^{2^J-1} X_{t-i}. \quad (\text{A.4})$$

Equations (2) - (4) illustrate how the original series  $X_t$ , exclusively defined in the time domain, can be decomposed into different time series components, each defined in the time domain and representing the fluctuation of the original time series in a specific frequency band. As in the Beveridge and Nelson (1981) time-series decomposition into stochastic trends and transitory components, the wavelet coefficients  $D_{j,t}$  can be viewed as components with different levels of calendar-time persistence operating at different frequencies; whereas the scaling coefficient  $S_{J,t}$  can be interpreted as the low-frequency trend of the time series under analysis. In particular, when  $j$  is small, the  $j$  wavelet coefficients represent the higher frequency characteristics of the time series (i.e., its short-term dynamics). As  $j$  increases, the  $j$  wavelet coefficients represent lower frequencies movements of the series.

### A.3 The Wavelet Transform: A Simple Example

The wavelet coefficients resulting from the MODWT with Haar filter are fairly straightforward to interpret as they are simply differences of moving averages. Consider the case of  $J = 1$ . A time series  $X_t$  is then decomposed into a transitory component  $D_1$  and a persistent scale component  $S_1$  as:

$$X_t = \underbrace{\frac{X_t - X_{t-1}}{2}}_{D_{1,t}} + \underbrace{\frac{X_t + X_{t-1}}{2}}_{S_{1,t}}. \quad (\text{A.5})$$

When  $J = 2$ , the decomposition results in two detail components  $D_1$  and  $D_2$  and a scale component  $D_1$ :

$$X_t = \underbrace{\frac{X_t - X_{t-1}}{2}}_{D_{1,t}} + \underbrace{\frac{X_t + X_{t-1} - (X_{t-2} + X_{t-3})}{4}}_{D_{2,t}} + \underbrace{\frac{X_t + X_{t-1} + X_{t-2} + X_{t-3}}{4}}_{S_{2,t}}. \quad (\text{A.6})$$

While the first component  $D_1$  remains unchanged at the now higher scale  $J = 2$ , the prior persistent component  $S_1$  is divided into an additional transitory component  $D_2$  and a new persistent one  $S_2$ . The length  $K_j$  of the filter, that is, the number of observations needed to compute the coefficients, increases with  $j$ :  $K_j = 2^j$ . Hence, the coarser the scale, the longer the filters. Intuitively, the lower the frequencies a researcher wants to capture, the wider the time window to be considered. Alternatively, the lower the frequencies targeted, the longer the data sample required. The equations also show that this is a one-sided filter, as future values of  $X_t$  are not needed to compute the coefficients of the wavelet transform of  $X_t$  at time  $t$ . This implies that the  $D_{j,t}$  and  $S_{j,t}$  lag  $X_t$ . In other words, they reflect the changes in  $X_t$  with some delay. Moreover, since the length of the filters increases with  $j$ , so does the delay. Hence, the coarser the scale, the more the wavelet components are lagging behind  $X_t$ . Finally, the scale of the decomposition is related to the frequency at which activity in the time series occurs. For example, with annual or quarterly time series, Table A.1 shows the interpretation of the different scales.

Table A.1: Scales and Cycle Length

Scale $j$	Period Length	
	Annual Data	Quarterly Data
1	2y-4y	2q-4q
2	4y-8y	4q-8q=1y-2y
3	8y-16y	8q-16q=2y-4y
4	16y-32y	16q-32q=4y-8y
5	32y-64y	32q-64q=8y-16y
6	64y-128y	64q-128q=16y-32y
...	>128y	>128q=32y

## B Data

We extract aggregate time series from the Haver database. The data are collected quarterly and cover the period from 1954Q3 to 2017Q3, which is the longest available time span for the variables we consider. Table B1 reports further details on the data, while Figure B1 shows the raw data series. We report results for GDP growth, which we compute as the quarter-over-quarter rate. Similarly, our measure of inflation is the quarter-over-quarter growth rate of the PCE price index. We also construct a time series for the spread between the long and the short bond rate, computed as the simple difference.

Table B1: Data

Variable	Mnemonic	Comment
Real GDP	GDPH@USECON	Seasonally Adjusted
Unemployment	LR@USECON	Seasonally Adjusted, 16 and over
PCE Price Index	JC@USECON	Seasonally Adjusted
Federal Funds Rate	FFED@USECON	Monthly Average of Daily Data
3-Month Treasury Rate	FTBS3@USECON	Monthly Average of Daily Data
10-Year Treasury Rate	FCM10@USECON	Monthly Average of Daily Data

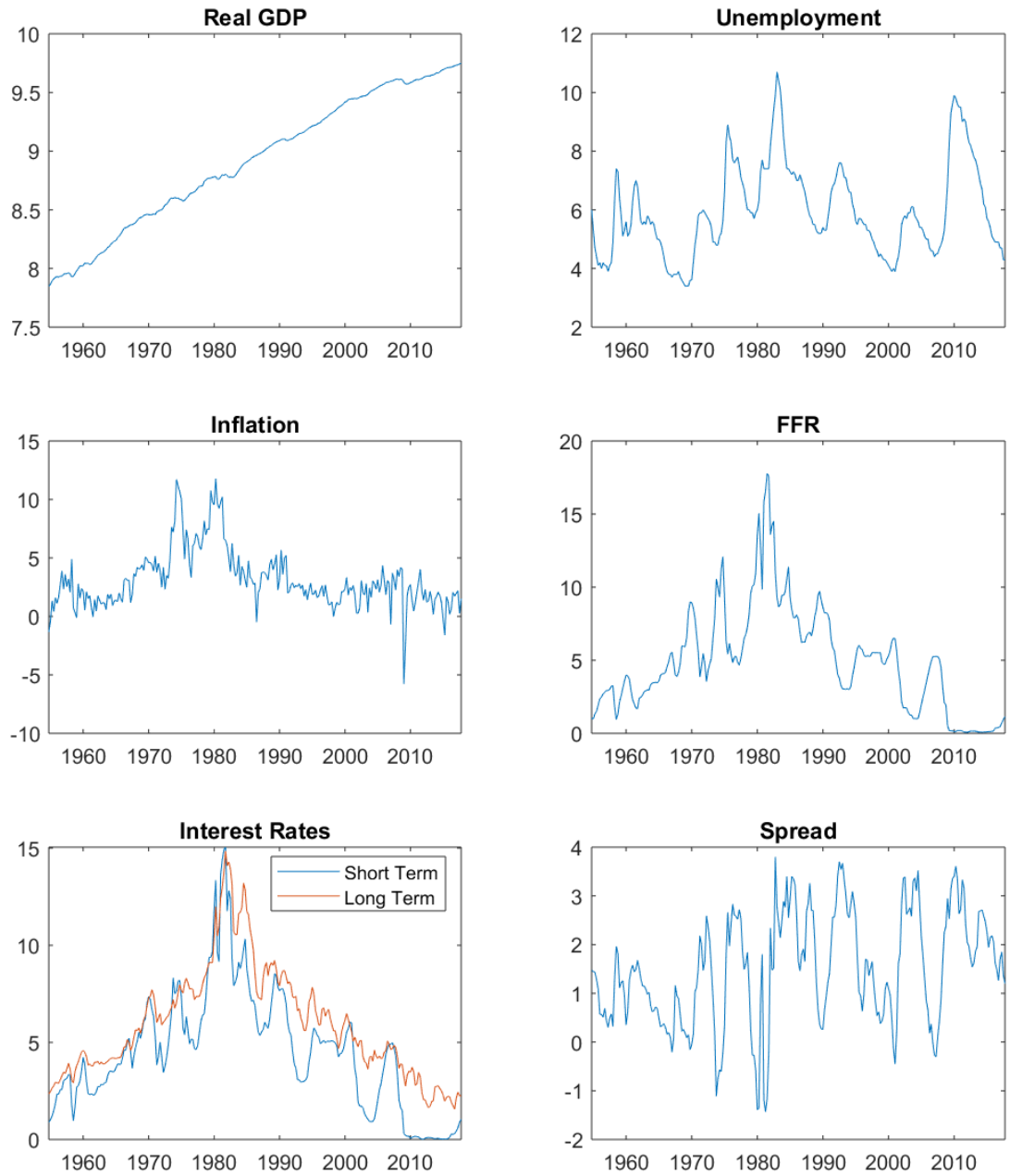


Figure B1: Macroeconomic Time Series Data

## C Additional Wavelet Decompositions

### C.1 One-Sided Haar Filter

The figures in this section report the wavelet components  $D_1 - D_6$  and the scale component  $S_6$  individually for each of the six macroeconomic time series and for the term spread, the difference between the 10-year and the 3-month rate. In the figures, we show the respective component in dark blue against the overall underlying data series in grey.

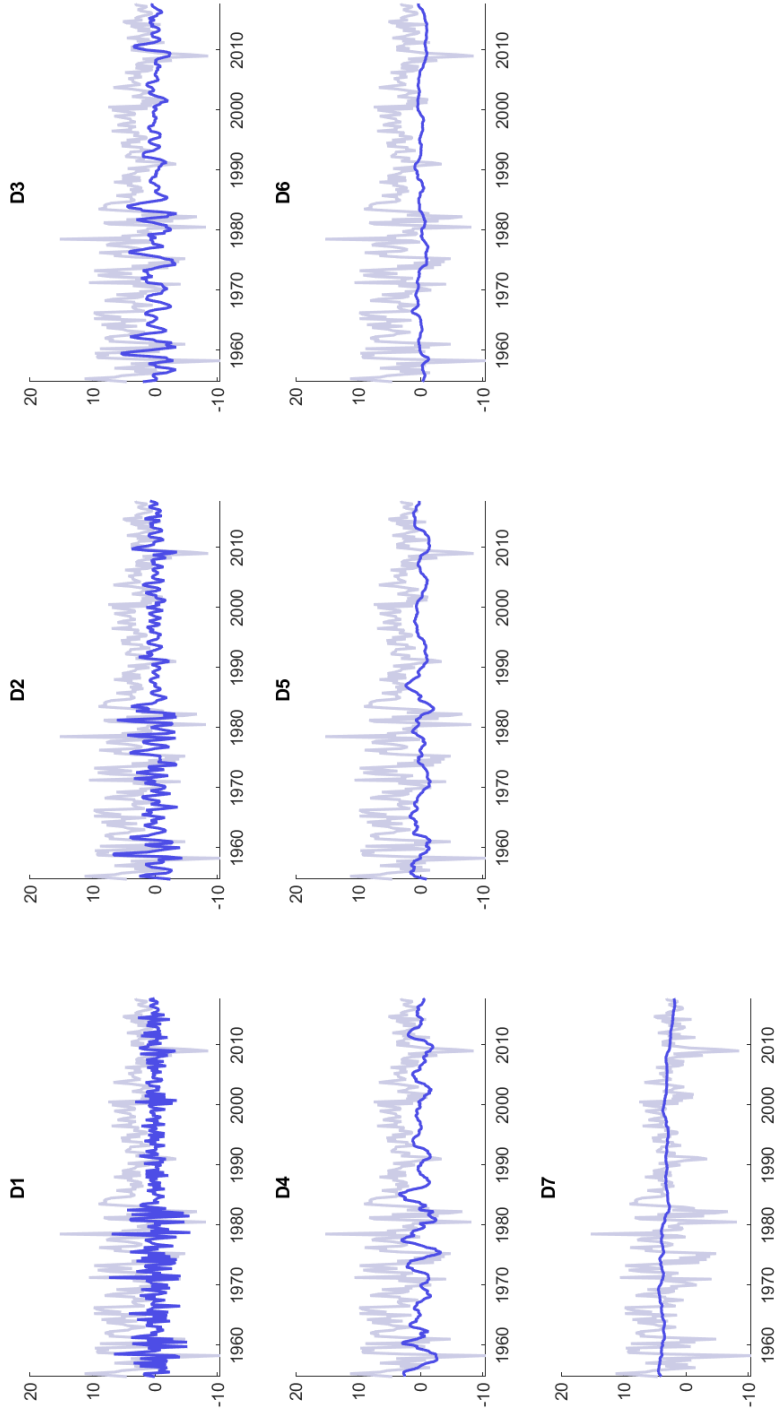


Figure C.1: One-Sided Haar Filter Wavelet Decomposition: Real GDP Growth

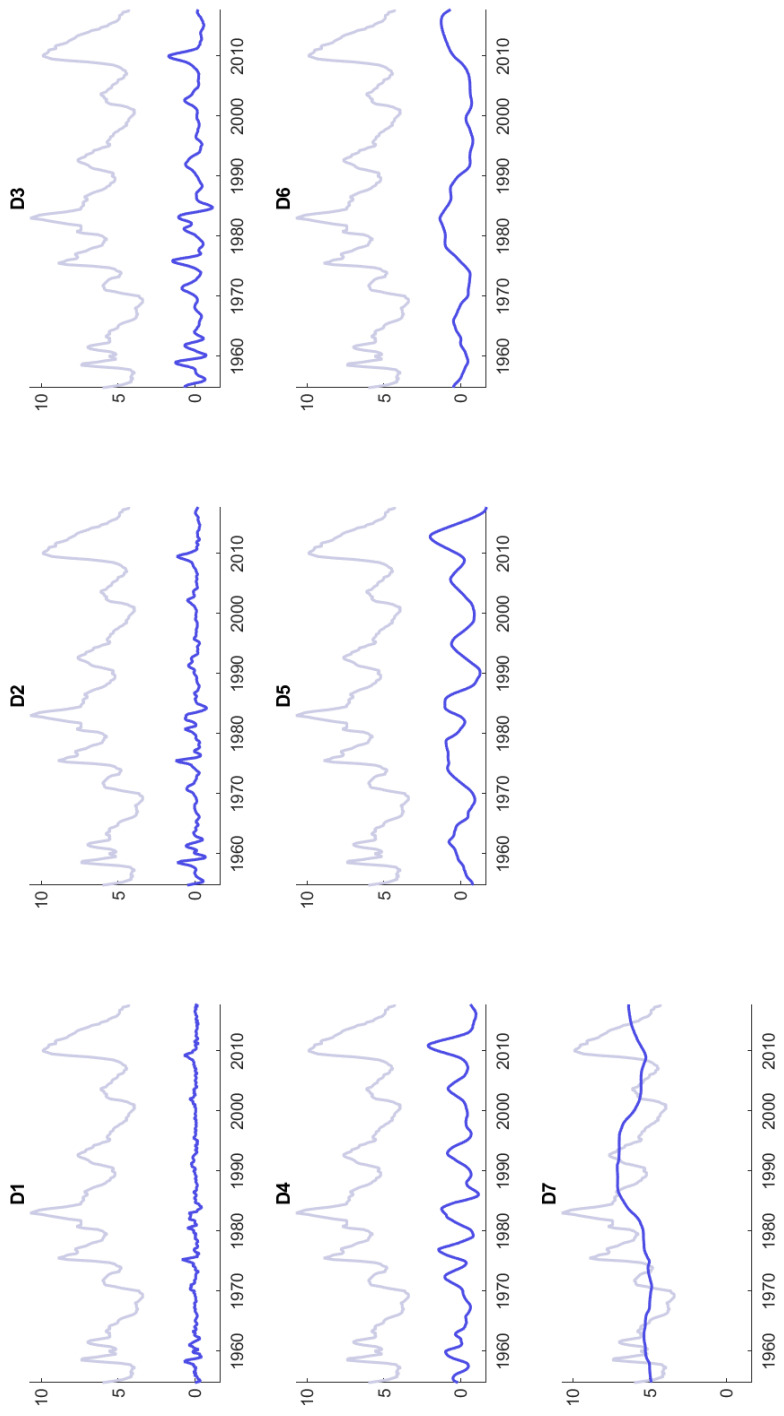


Figure C.2: One-Sided Haar Filter Wavelet Decomposition: Unemployment

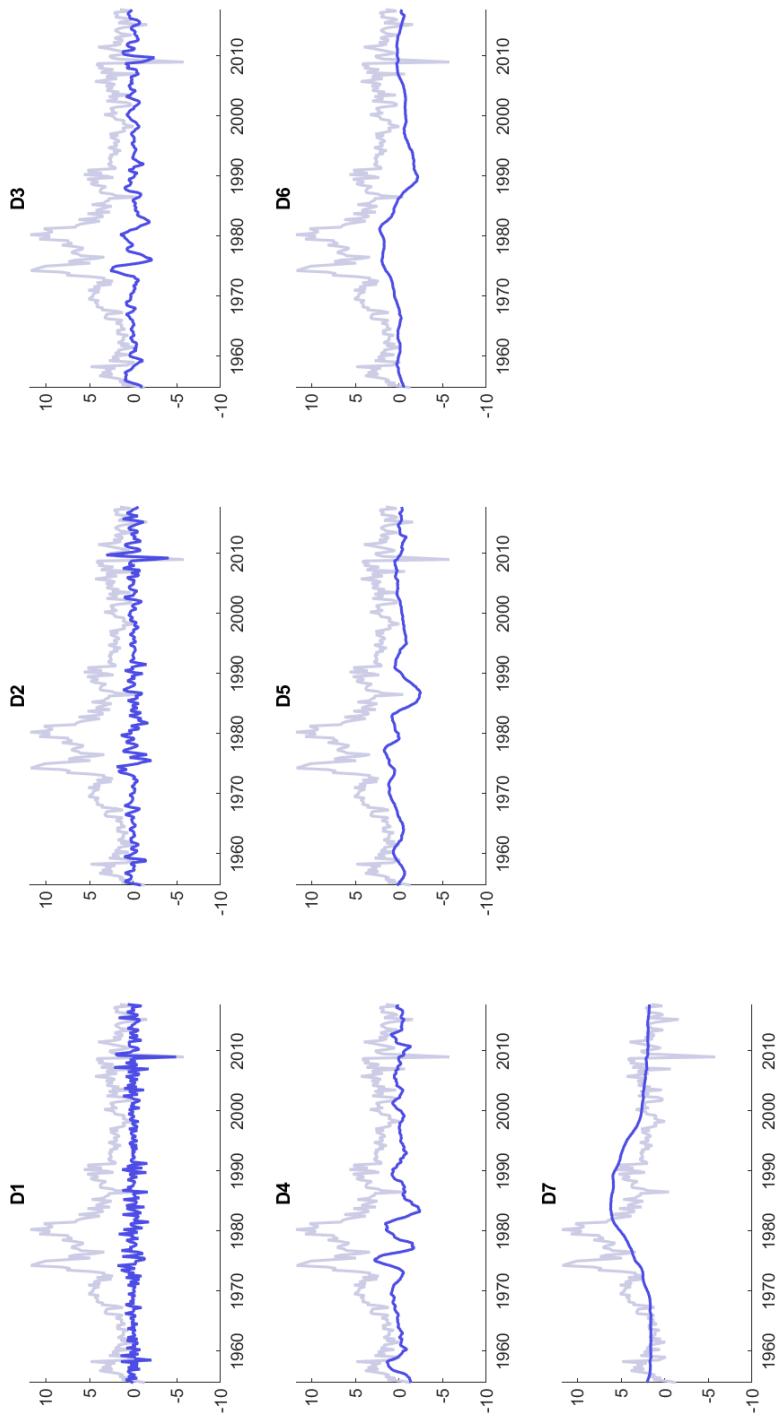


Figure C.3: One-Sided Haar Filter Wavelet Decomposition: Inflation

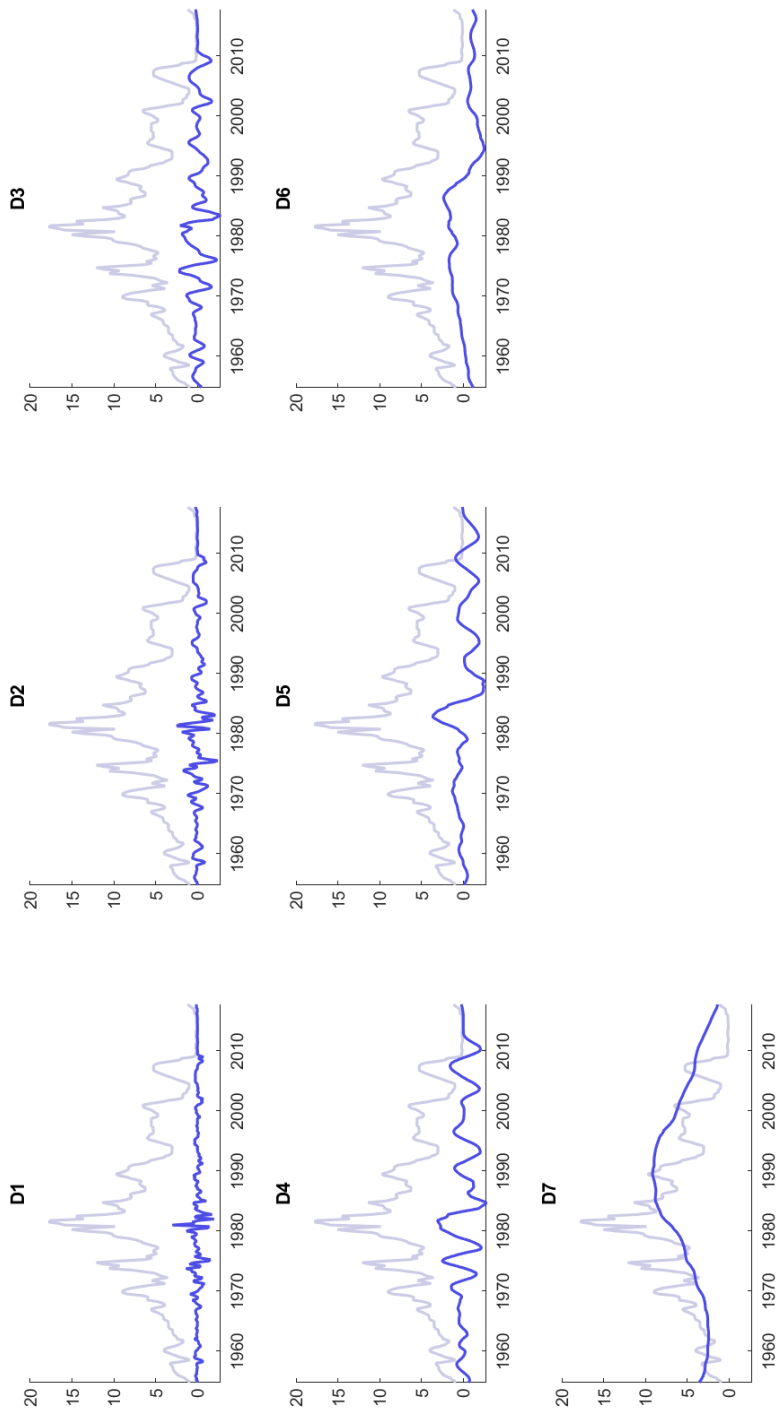


Figure C.4: One-Sided Haar Filter Wavelet Decomposition: Federal Funds Rate

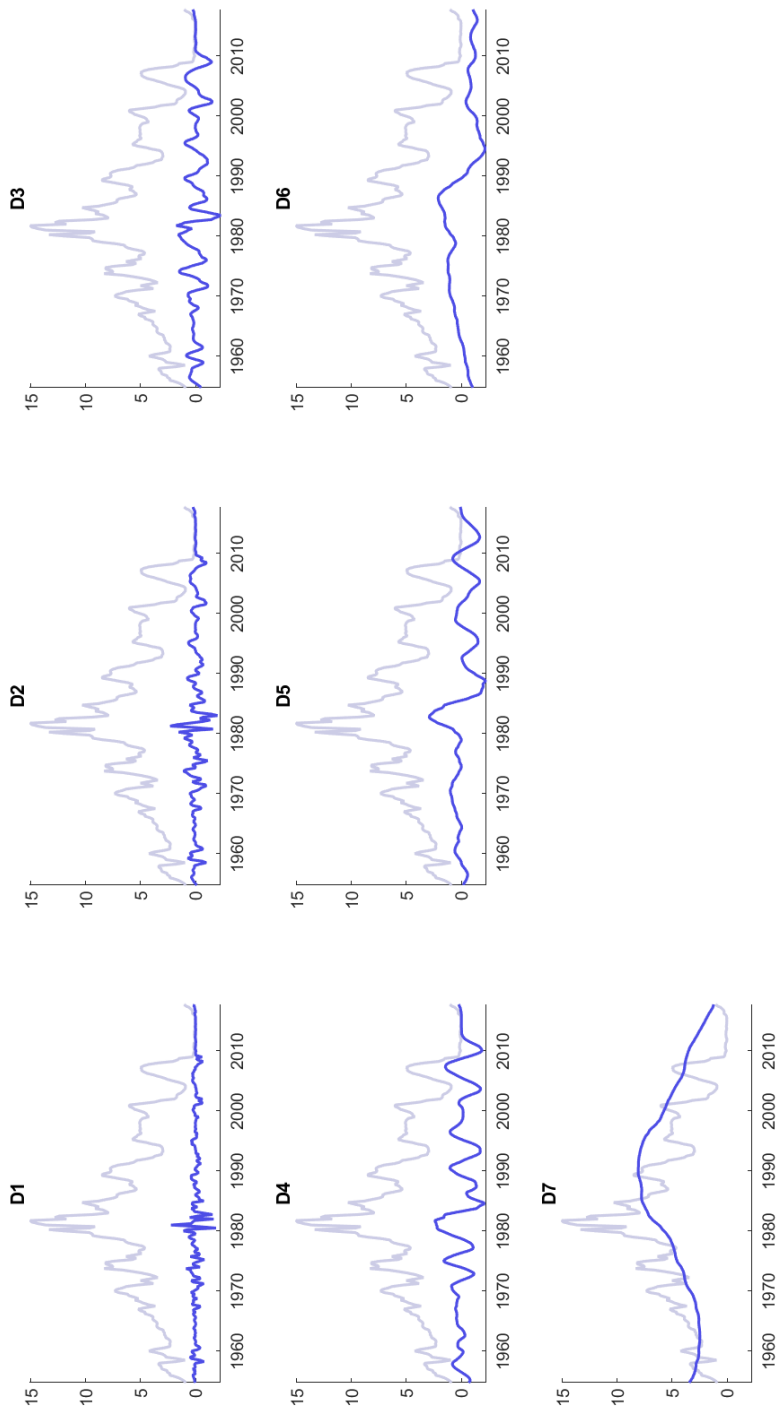


Figure C.5: One-Sided Haar Filter Wavelet Decomposition: 3-Month Treasury Rate

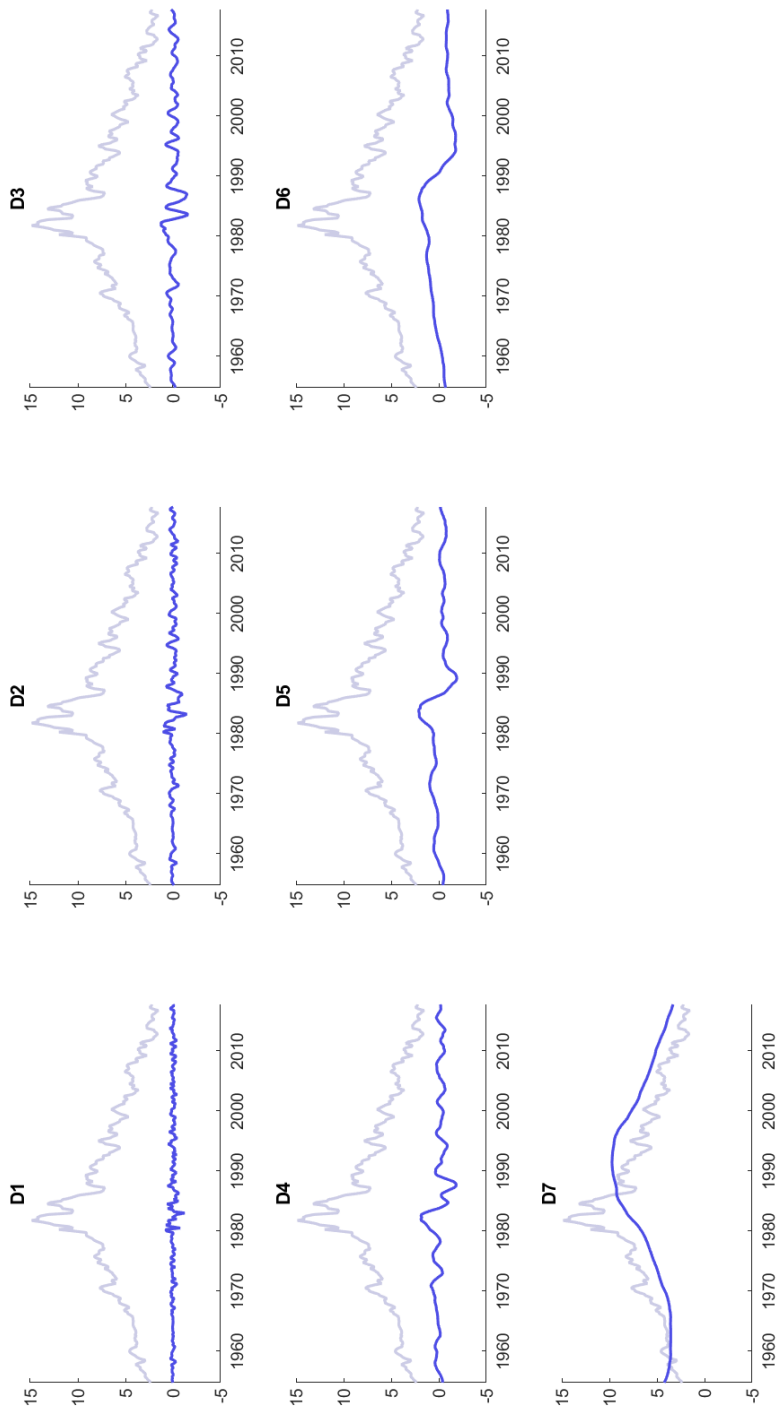


Figure C.6: One-Sided Haar Filter Wavelet Decomposition: 10-Year Treasury Rate

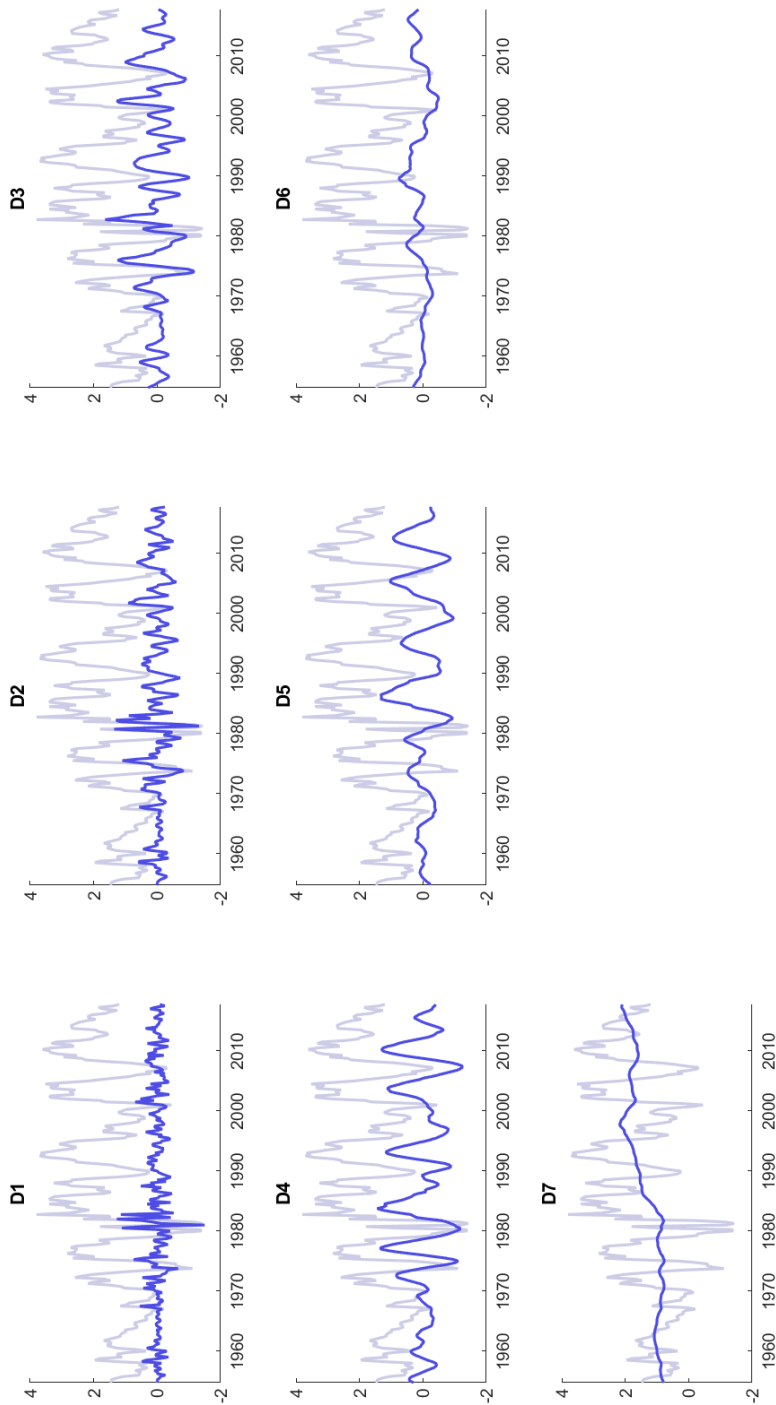


Figure C.7: One-Sided Haar Filter Wavelet Decomposition: Term Spread

## C.2 One-Sided Daubechies Filter

The figures in this section report the wavelet decompositions for the four categories ‘Short Term’ ( $D_1, D_2$ ), ‘Business Cycle’ ( $D_3, D_4$ ), ‘Medium Term’ ( $D_5, D_6$ ), and ‘Long Term’ ( $S_6$ ) from a decomposition that uses the Daubechies wavelet filter. We report the decompositions for inflation, the federal funds rate, and the 10-year rate. For comparison purposes, the figures also report the corresponding Haar-filter decompositions.

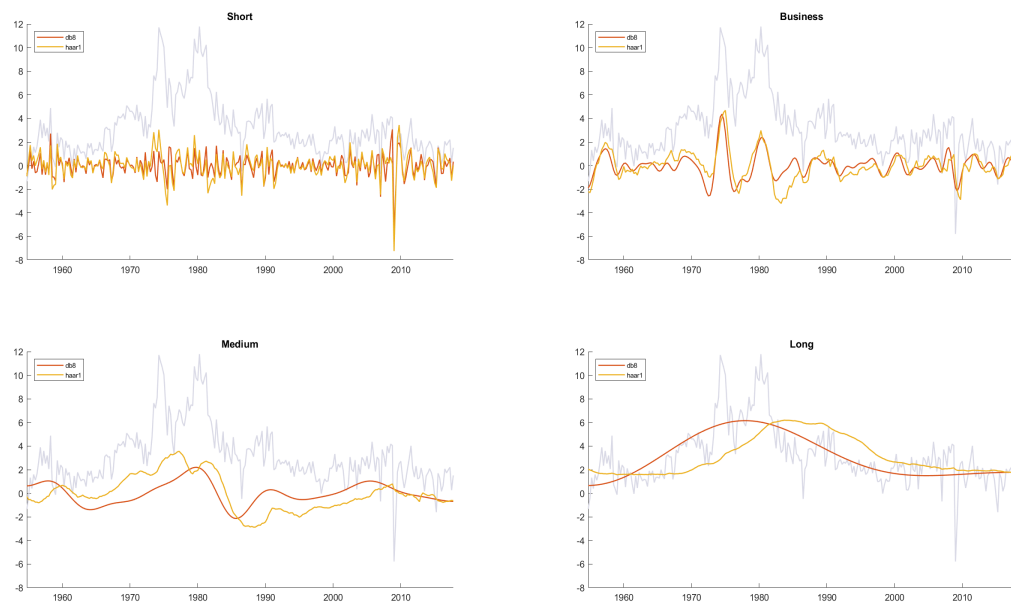


Figure C.8: Wavelet Decompositions for Alternative Filters: Inflation

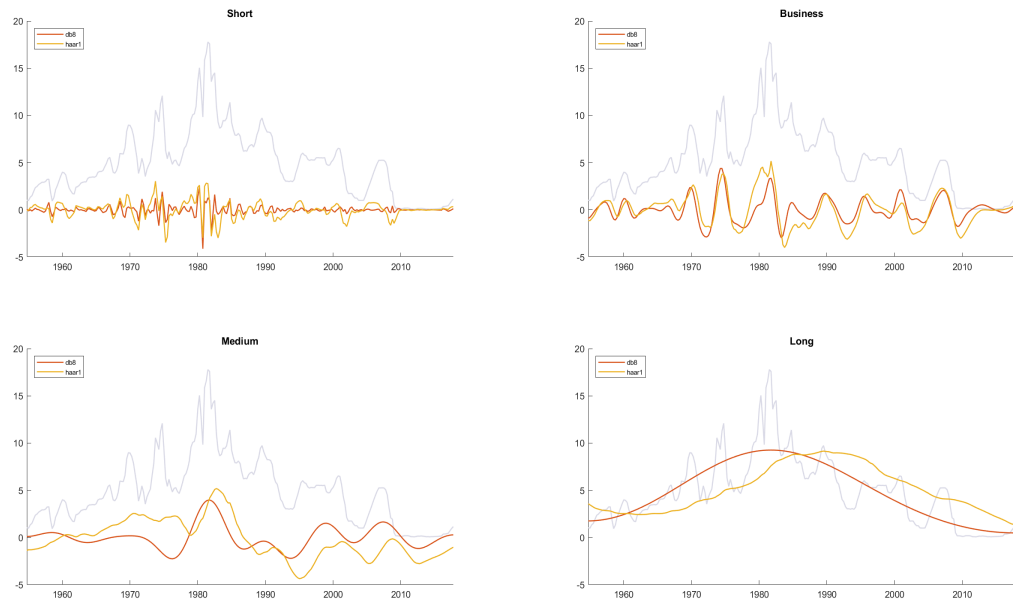


Figure C.9: Wavelet Decompositions for Alternative Filters: Federal Funds Rate

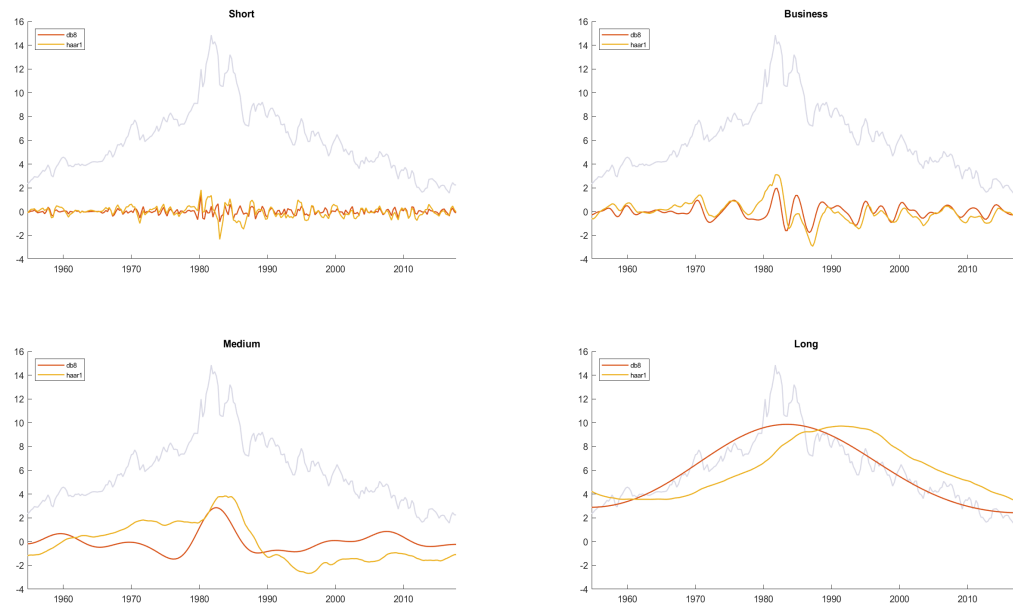


Figure C.10: Wavelet Decompositions for Alternative Filters: 10-Year Treasury Rate

## D The Frequency-Specific Effects of Monetary Policy Shocks

### D.1 VAR Specification

We closely follow Arias et al. (2018) in the specification and estimation of a structural VAR (SVAR) to identify the effects of a monetary policy shock. Specifically, we estimate an SVAR of the following form:

$$y_t' A_0 = c + \sum_{l=1}^L y_{t-l}' A_l + \varepsilon_t'. \quad (\text{A.7})$$

$y_t$  is a column vector that collects the observable variables, and  $\varepsilon_t$  collects the structural innovations;  $c$  is a vector of constants, while  $L$  is the number of lags in the VAR. Our focus is on determining the elements in the structural impact matrix  $A_0$ . Since we do not impose overidentifying restrictions, we can estimate the reduced-form VAR and impose our identification restrictions after estimation. To do so, we post-multiply the previous equation by  $A_0^{-1}$  to arrive at:

$$y_t' = x_t' B + u_t', \quad (\text{A.8})$$

where  $x_t$  also contains the intercept term. We use conjugate Normal-inverse Wishart priors of the form used in Arias et al. (2018). We assume four lags and a loose, but proper, prior throughout. Once we have parameter estimates for  $B$  and the covariance matrix of  $u_t$ , we follow the algorithm outlined in Rubio-Ramirez et al. (2010) to impose sign restrictions on impact. With respect to the latter, we assume that the level of the nominal rate increases on impact after a monetary policy shock, inflation decreases, and either that (i) the unemployment rate increases or (ii) that real GDP growth decreases, given the activity variable used in the estimation.

### D.2 Impulse Response Functions

In this section we report the impulse response functions based on unemployment as the macroeconomic activity variable in the VAR. Specifically, we report results from a specification where we add the short-term  $D_2$ , the business-cycle  $D_4$ , and the long-term  $S_6$  component.

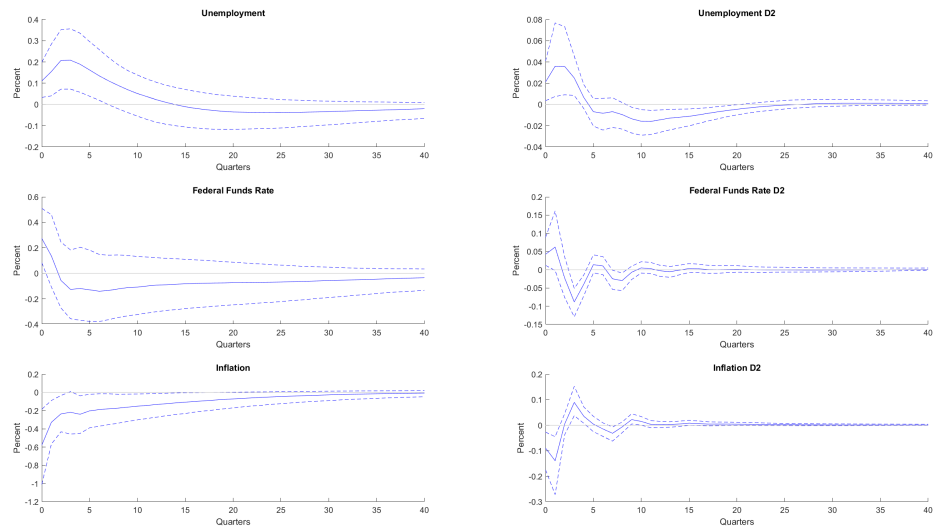


Figure D.1: Impulse Response Functions with  $D_2$  Components

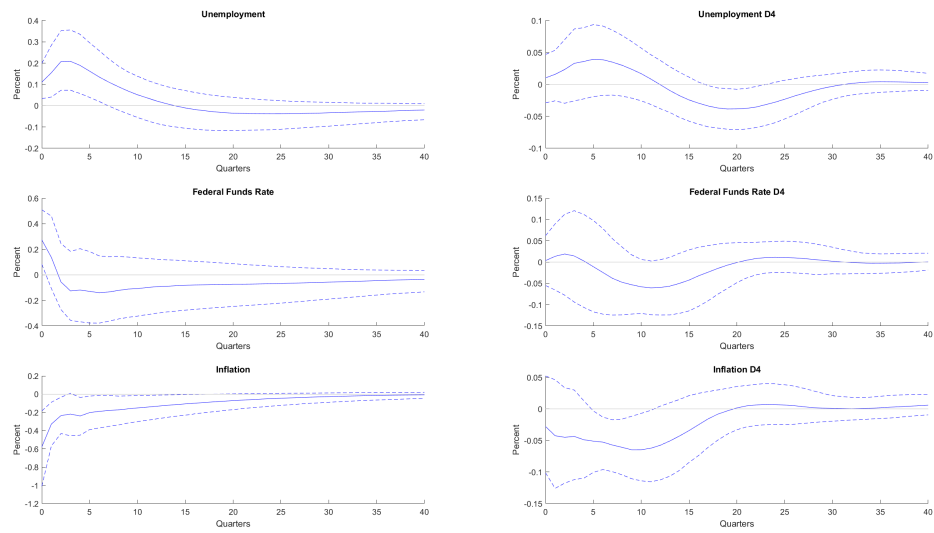


Figure D.2: Impulse Response Functions with  $D_4$  Components

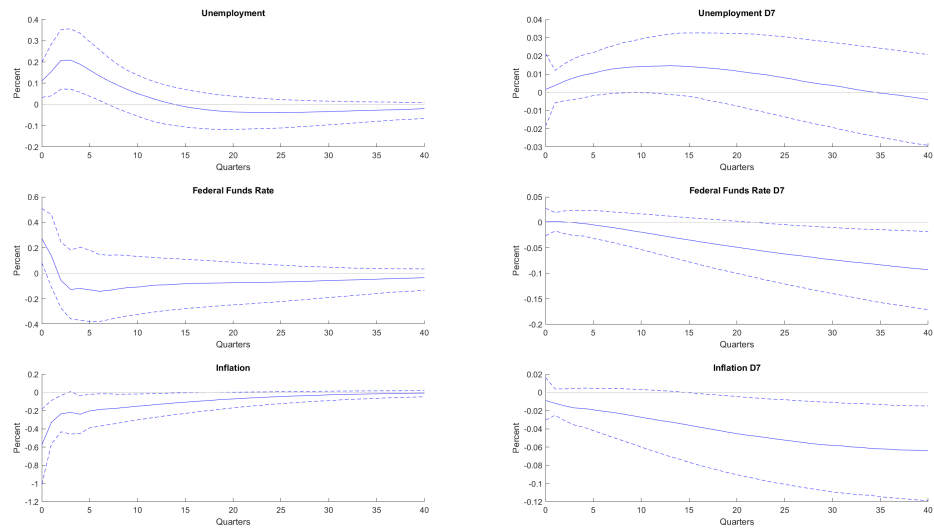


Figure D.3: Impulse Response Functions with  $S_6$  Components

## References

- [1] Arias, Jonas E., Juan F. Rubio-Ramírez, and Daniel F. Waggoner (2018): “Inference Based on Structural Vector Autoregressions Identified With Sign and Zero Restrictions: Theory and Applications”. *Econometrica*, 86(2), pp. 685-720.
- [2] Baxter, Marianne, and Robert G. King (1999): “Measuring Business Cycles: Approximate Band-Pass Filters for Economic Time Series”. *The Review of Economics and Statistics*, 81(4), pp. 575-593.
- [3] Beveridge, Stephen, and Charles R. Nelson (1981): “A New Approach to Decomposition of Economic Time Series into Permanent and Transitory Components with Particular Attention to Measurement of the ‘Business Cycle’ ”. *Journal of Monetary Economics*, 7(2), pp. 151-174.
- [4] Hodrick, Robert, and Edward C. Prescott (1997): “Postwar U.S. Business Cycles: An Empirical Investigation”. *Journal of Money, Credit, and Banking*, 29(1), pp. 1-16.
- [5] Rubio-Ramírez, Juan F., Daniel F. Waggoner, and Tao Zha (2010): “Structural Vector Autoregressions: Theory of Identification and Algorithms for Inference”. *Review of Economic Studies*, 77(2), pp. 665-696.
- [6] Watson, Mark W. (1986): “Univariate Detrending Methods with Stochastic Trends”. *Journal of Monetary Economics*, 18, pp. 49-75.